American Journal of Pathology, Vol. 153, No. 3, September 1998

Multistep Nature of Metastatic Inefficiency

Dormancy of Solitary Cells after Successful Extravasation and Limited Survival of Early Micrometastases

Keith J. Luzzi,* Ian C. MacDonald,* Eric E. Schmidt,* Nancy Kerkvliet,† Vincent L. Morris,*‡§ Ann F. Chambers,*†‡§ and Alan C. Groom*

From the Departments of Medical Biophysics, Microbiology and Immunology,‡ and Oncology,§ University of Western Ontario, London Regional Cancer Centre,† London, Ontario, Canada*

In cancer metastasis, only a small percentage of cells released from a primary tumor successfully form distant lesions, but it is uncertain at which steps in the process cells are lost. Our goal was to determine what proportions of B16F1 melanoma cells injected intraportally to target mouse liver 1) survive and extravasate, 2) form micrometastases (4 to 16 cells) by day 3, 3) develop into macroscopic tumors by day 13, and 4) remain as solitary dormant cells. Using *in vivo* videomicroscopy, a novel cell accounting assay, and immunohistochemical markers for proliferation (Ki-67) and apoptosis (TUNEL), we found that 1) 80% of injected cells survived in the liver microcirculation and extravasated by day 3, 2) only a small subset of extravasated cells began to grow, with 1 in 40 forming micrometastases by day 3, 3) only a small subset of micrometastases continued to grow, with 1 in 100 progressing to form macroscopic tumors by day 13 (in fact, most micrometastases disappeared), and 4) 36% of injected cells remained by day 13 as solitary cancer cells, most of which were dormant (proliferation, 2%; apoptosis, 3%; in contrast to cells within macroscopic tumors: proliferation, 91%; apoptosis/necrosis, 6%). Thus, in this model, metastatic inefficiency is principally determined by two distinct aspects of cell growth after extravasation: failure of solitary cells to initiate growth and failure of early micrometastases to continue growth into macroscopic tumors. *(Am J Pathol 1998, 153:865–873)*

The metastatic spread of cancer cells from a primary tumor to distant sites in the body is responsible for most cancer patient morbidity and mortality.[1–3] Fortunately, the metastatic process is inefficient[4] in that very few of the tumor cells released into the circulation develop into metastases; experimental studies have shown that only ~0.01% of cancer cells injected into the circulation form metastatic foci (See, eg, Ref. 5). It is uncertain at which steps in the process cells are lost, but it has generally been thought that most cancer cells are rapidly destroyed in the circulation (eg, Ref. 5), either by the immune system[6,7] or hemodynamic forces.[8] In addition, the ability of cells to extravasate into the surrounding tissue, by degrading basement membrane and extracellular matrix, has been considered another major rate-limiting step in metastasis.[4,9] However, we have demonstrated quantitatively that virtually all injected melanoma cells survive in the microcirculation and successfully extravasate by 24 hours after injection in chick embryo chorioallantoic membrane (CAM).[10] Furthermore, in the same model we have shown that extravasation is independent of metastatic ability, for *ras*-transformed and control fibroblasts extravasate equally well.[11] Together, our studies imply that the primary determinants of metastatic inefficiency are the post-extravasation survival and growth of cells,[12] but whether this conclusion may be generalized to mammalian models remains uncertain.

Our goal in the present study was to investigate the multistep nature of metastatic inefficiency in a mouse liver model, by quantifying what proportions of B16F1 melanoma cells injected intraportally 1) survive and extravasate, 2) divide and form micrometastases, 3) develop into macroscopic tumors, and 4) remain as solitary dormant cells. We used *in vivo* videomicroscopy[12,13] to observe individual cells directly and quantify cell extravasation, a novel cell accounting assay to quantify the survival of injected cancer cells,[10] and immunohistochemistry to assess proliferation (Ki-67) and apoptosis (TUNEL). We found that >80% of the injected cells survived and had extravasated by day 3. However, few extravasated cells began to grow, with only 1 in 40 forming micrometastases (4 to 16 cells) by day 3. Furthermore, few micrometastases continued to grow, with only 1 in 100 progressing to form macroscopic tumors by day 13; in fact, by then most micrometastases had disappeared. Surprisingly, 36% of

Supported by National Cancer Institute of Canada Grant 8133. A. F. Chambers is a Senior Scientist of Cancer Care Ontario.

Accepted for publication June 25, 1998.

Address reprint requests to Dr. Ann F. Chambers, The London Regional Cancer Centre, 790 Commissioners Road East, London, ON Canada N6A 4L6. E-mail: achambers@lrcc.on.ca.

injected cells remained by day 13 as solitary cancer cells, 95% of which were shown to be dormant; in contrast, within macroscopic tumors, only 3% of cells were dormant. Thus, in this model, metastatic inefficiency is principally determined by two distinct aspects of cell growth after extravasation: the failure of solitary cells to initiate growth and the failure of early micrometastases to continue growth into macroscopic tumors.

Materials and Methods

Cell Culture and Fluorescent Labeling

B16F1 murine melanoma cells[14] were maintained in tissue culture (37°C, 5% CO_2 humidified atmosphere) in Alpha minimal essential medium plus ribonucleosides (α-plus MEM; Life Technologies, Burlington, Ontario, Canada) supplemented with 10% fetal calf serum (FCS; Hyclone, Logan, UT). Cells were routinely subcultured as subconfluent monolayers every 3 days and were not kept in culture for more than five passages.

Cells for injection were fluorescently labeled (yellow-green) using Fluoresbrite carboxylated polystyrene nanospheres of 48 nm diameter (Polysciences, Warrington, PA). Nanospheres were prepared in a sterile, monodispersed suspension diluted 1:50 in Opti-MEM serum-reduced medium (Life Technologies). Cells were labeled by replacing the α-plus MEM with the nanosphere suspension for 1 hour as described previously.[15] All cells spontaneously incorporated these virus-sized fluorescent nanospheres into their cytoplasm and retained them.[10] Cells were harvested by trypsinization and resuspended in α-plus MEM/10% FCS to a final concentration of 1.5×10^6 cells/ml. Tests of the labeled cells showed that the labeling procedure does not affect the plating efficiency or growth of B16F1 cells *in vitro* or the metastatic behavior *in vivo*. Before injection, it was determined by fluorescence microscopy that ≥95% of the cells excluded ethidium bromide, indicating that membrane integrity was maintained.[10,16] Additionally, 10.2-μm-diameter microspheres were added to the cell suspension (~5:1 cells:microspheres) to allow for monitoring of cell survival as described in the cell accounting procedure given below.

Experimental Metastasis Assay

Female C57Bl/6 mice (Harlan Sprague-Dawley, Indianapolis, IN) aged 6 to 8 weeks, syngeneic to B16F1 cells, were cared for in accordance with standards of the Canadian Council on Animal Care, under an approved protocol of the University of Western Ontario Council on Animal Care. Mice were anesthetized using a ketamine/xylazine mixture (1.6 mg of ketamine and 0.08 mg of xylazine per 15 g of body mass) administered by intraperitoneal injection. A suspension of 3×10^5 fluorescently labeled B16F1 cells and 6×10^4 microspheres in 0.2 ml of α-plus MEM supplemented with 10% FCS was injected into the superior mesenteric vein of each mouse to target the liver as described.[13] Buprenorphrine analgesic (0.02 to 0.04 mg/kg) was administered subcutaneously as mice awoke and also 18 hours after surgery.

At 13 days after injection, mice were sacrificed by CO_2 asphyxiation. Livers were examined for visible surface tumors (mass, tumor number, and tumor size) and then fixed in 10% neutral buffered formalin (pH 7.6). Three of the livers were randomly chosen and grossly sectioned (~1 mm thick) using a scalpel to determine whether there were any tumors present in the interior that were not visible when examining the liver surface. The remaining livers were examined using the cell accounting procedure described below.

Intravital Videomicroscopy

The procedure for intravital videomicroscopy of mouse liver has been described previously.[12,17] Briefly, mice were anesthetized with sodium pentobarbitol (60 mg/kg intraperitoneally), after which the liver was exposed and the mouse placed on a viewing platform on the stage of an inverted epifluorescence microscope (Nikon Diaphot TMD). A fiber optic light source provided oblique transillumination, resulting in high-contrast views of the liver microvasculature along with associated cells and tissues. Images were obtained using a video camera, viewed on a video monitor, and recorded on SVHS videotape. Body temperature was monitored and maintained at 37°C, and anesthesia was maintained with supplemental administration of sodium pentobarbitol as required. At the end of each experiment, the animal was killed by anesthetic overdose, and the liver was removed and fixed in 10% neutral buffered formalin.

Mice that had been injected with cancer cells, as described above for the experimental metastasis assay, were observed at either of two time points: immediately (15 to 90 minutes) after injection or 3 days later. The injected B16F1 cells were assessed as being wholly intravascular, in the process of extravasating, or extravascular. Individual cells were positively identified by their fluorescence and/or melanin content. Intravital videomicroscopy was also used for cell accounting[10] (see below) in the superficial regions of the liver, as it is possible to optically slice to a depth of ~50 μm below the surface. The numbers of multicellular foci (4 to 16 cells) present at day 3 were also quantified. Although other workers have previously visualized such early micrometastases from *lacZ*-transfected gastric carcinoma cells using β-galactosidase-stained liver sections,[18] in the present study we were able to quantify early micrometastases *in vivo*, visible due to their melanin content, using intravital videomicroscopy.

Cell Accounting in Tissues

To determine the proportions of the injected cancer cells that extravasate and survive in the tissue, form micrometastases, or develop into tumors, it is necessary to express the number observed in a tissue sample relative to the number of cells originally entering that volume. We recently developed a cell accounting technique for this

purpose, based on the standard method for measuring distribution of blood flow,[19] and used it with *in vivo* videomicroscopy to determine the 24-hour survival of melanoma cells in chick embryo CAM.[10] Inert microspheres (nonfluorescent) that remain trapped by size restriction within the microcirculation are injected together with the cancer cells, providing a reference standard for monitoring cell survival at various times later. In mouse liver, cancer cells injected intraportally become arrested by size restriction in periportal sinusoids,[13] which have a diameter of 5.9 ± 0.87 μm (mean ± SD).[20] Therefore, to ensure trapping of all of the reference microspheres in sinusoids, the microspheres should be not less than ~8.5 μm in diameter. (This size represents 3 SDs above sinusoidal mean diameter, and therefore only 1 in 1000 vessels would be expected to allow a microsphere to pass through.) We were able to obtain 10.2-μm polystyrene microspheres with a very narrow range of diameters (±0.1 μm SD; Bangs Laboratories, Fishers, IN), and using *in vivo* videomicroscopy we verified, by direct observation, that all microspheres entering the liver microcirculation after intraportal injection immediately became trapped in sinusoids. No microspheres were ever observed passing through the sinusoids to the hepatic venous outflow.

To confirm that the microspheres remained trapped in the liver on a long-term basis, livers from four mice at each of three different time points (90 minutes and 3 and 13 days after injection) were examined to determine whether the number of microspheres per unit volume of tissue stayed constant over time. Formalin-fixed livers were cut to 30-μm-thick sections using a Vibratome Series 1000 sectioning system (Technical Products International, St. Louis, MO). Sections were mounted on a number 1 coverglass and viewed using the microscope described above. One section from each lobe of the liver was analyzed to count the number of microspheres. The 10.2-μm nonfluorescent microspheres were readily seen due to their high refractive index as well as their distinctive spherical shape. The area, and consequently the volume, of each section was determined, allowing a microsphere density to be calculated.

For cell accounting experiments, microspheres were included in the melanoma cell suspension to be injected into the mouse, at a concentration of 3×10^5 microspheres/ml (~5:1 cells:microspheres). We estimate that after the injection (0.2 ml per mouse) less than 1% of all periportal sinusoids are blocked by a microsphere; no general disruption of blood flow occurs, as downstream sinusoids are supplied by collateral flow. To determine the exact ratio of cells:microspheres in the syringe before injection, a drop of the suspension was placed on a coverglass and the numbers of cells and microspheres observed in eight fields of view (20× objective) were recorded. Cells remained uniformly dispersed and cell clumping was not observed. Only those cells that maintained membrane integrity, tested by exclusion of ethidium bromide[10] (≥95%) were used in calculating the cell:microsphere ratio. To quantify the percentage of injected melanoma cells surviving in the liver, the cell:microsphere ratio in the organ at 90 minutes and 3 and 13 days after injection was compared with the ratio in the syringe before injection.[10] The percentage cell survival was calculated as the (cell:microsphere ratio in liver after injection)/(cell:microsphere ratio in syringe before injection) × 100.

To determine cell survival throughout the liver, at the three time points after injection, formalin-fixed livers were cut to 30-μm-thick sections and examined as described above; a minimum of four sections per liver, transecting the whole organ at different positions, were examined. The numbers of B16F1 cells and 10.2-μm microspheres, along with micrometastases present at days 3 and 13, were recorded. Individual melanoma cells were positively identified by their fluorescence and/or melanin content; micrometastases observed at days 3 and 13 always displayed melanin. It should be noted that it is the ratio of cells/microspheres that matters, not the actual numbers of cells or microspheres. The actual numbers counted will depend on the total areas of the sections of liver obtained, and there is typically a certain amount of variability in the distribution within the liver of any cell suspension injected intraportally. However, in our cell accounting procedure, this variability is controlled for by the coinjection of the microspheres with the cells. Confirmation of the technique using thick sections was accomplished by performing cell accounting *in vivo* using videomicroscopy immediately after injection and at day 3. This allowed for a comparison of cell survival values determined from intact livers *in vivo versus* those from liver sections. Whenever multicellular foci were observed, either as micrometastases or macroscopic tumors, it was assumed that they originated from a single cell, as metastases have been shown to be clonal in origin.[21–23] Thus, the percent cell survival data obtained for days 3 and 13 represent minimal values.

Immunohistochemistry

Livers from three mice that had been injected with B16F1 cells 2 weeks previously (as described above) were fixed in 10% NB formalin for 24 hours and embedded in paraffin according to standard histological procedures. Serial sections (4 μm) were cut from two blocks from each liver and stained as follows: section 1 with Harris' hematoxylin and eosin (H&E), section 2 using the TUNEL assay (TdT-mediated dUTP nick-end-labeling) to assess apoptosis, section 3 with S100 (polyclonal antibody; Dako Z311) to identify melanoma cells, and section 4 with Ki-67 (monoclonal antibody; Novocastra NCL-Ki67-MM1) to assess proliferation. First, the sections stained with S100 were examined to identify melanoma cells. These cells were then assessed in the adjacent serial sections for markers of apoptosis and proliferation. Eight such sets of serial sections were examined from each tissue block, the six blocks yielding a total of 48 sections for each stain. The percentages of melanoma cells staining positive for TUNEL or Ki-67 were determined for 1) solitary cells within the tissue and 2) cells within tumors.

TUNEL Assay (after Gavrieli et al[24])

Deparaffinized sections were pretreated with proteinase K (20 μg/ml) for 15 minutes, endogenous peroxidase was inactivated using 3% hydrogen peroxide in methanol for 3 minutes, TdT (0.3 U/μl) and biotinylated dUTP were added, and the sections were incubated at 37°C for 60 minutes. Extra avidin peroxidase was applied for 30 minutes at 37°C. The sections were stained using an AEC (3-amino-9-ethylcarbazole) kit (Sigma), including a positive control that had been treated with DNAse I.

Ki-67 Staining[25]

Deparaffinized sections were pretreated two times in a microwave oven for antigen retrieval (3 minutes on high power and 7 minutes on low power in 10 mmol/L citrate buffer), 3% hydrogen peroxide was used to block endogenous peroxidase activity, nonspecific binding was blocked by incubating slides with normal goat serum, Ki-67 antibody was applied (1/150 dilution) overnight at room temperature, and positive staining was detected by incubating with a biotinylated secondary antibody followed by streptavidin-biotin peroxidase complex, according to the manufacturer's protocol (LSAB2 kit, Dako). Slides were counterstained with Mayer's hematoxylin. Positive and negative controls were also included.

S100 Staining[26]

The same protocol was followed as for Ki-67, except that the Envision kit (Dako), employing peroxidase-labeled polymer conjugated to anti-mouse and anti-rabbit immunoglobulins, replaced biotinylated secondary antibody and streptavidin peroxidase reagents. A 1/400 dilution of the primary antibody was applied for 2 hours.

Statistical Analysis

Statistical analysis was performed using SigmaStat for Windows v1.0 (Jandel Scientific, San Rafael, CA). All analyses were based on the number of mice. Differences between means were determined using the *t*-test when groups passed both a normality test and an equal variance test. When this was not the case, the Mann-Whitney rank sum test was used. A one-way analysis of variance was used to test whether the number of microspheres per unit volume of liver tissue changed with time. A level of $P < 0.05$ was regarded as statistically significant.

Results

To investigate the multistep nature of metastatic inefficiency in the mouse liver model, we quantified cell arrest and extravasation using intravital videomicroscopy, determined survival of cells and micrometastases by means of a cell accounting assay using reference microspheres, and assessed dormancy of cells by immunohistochemistry.

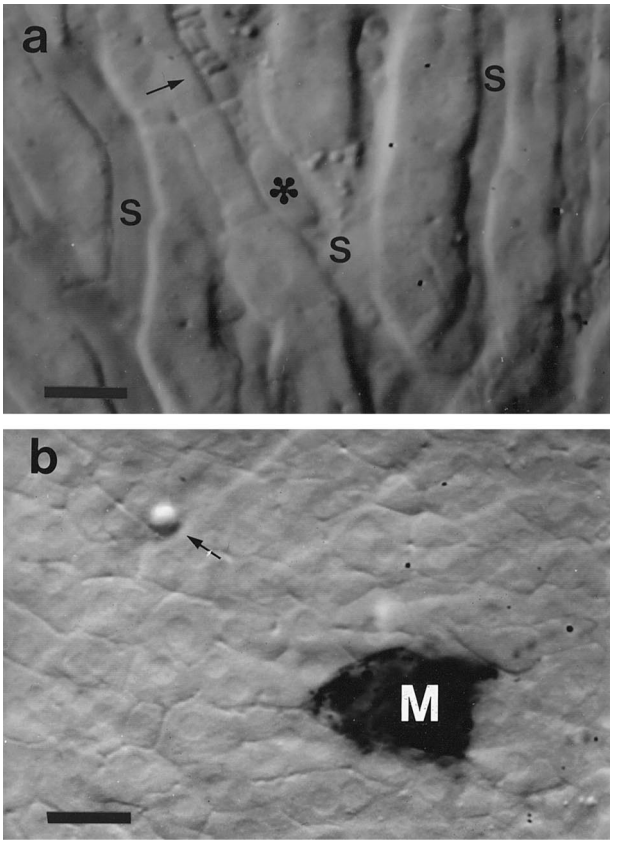

Figure 1. Intravital videomicroscopic views of B16F1 melanoma cells in mouse liver. a: Intravascular melanoma cell (*) arrested due to size restriction within a sinusoid (S), shown 45 minutes after injection. Blood flow is blocked (→) in the region immediately downstream from the cell; sinusoids further downstream are being supplied by collateral flow. b: Micrometastasis (M) at the liver surface 3 days after cell injection, displaying melanin. A microsphere (→), slightly below the plane of focus, is also visible. Scale bars, 20 μm.

Cell Arrest and Extravasation

The fate of melanoma cells immediately after intraportal injection and 3 days later was studied by direct observation *in vivo* using videomicroscopy. All cells became arrested by size restriction in liver sinusoids of acinar zone 1, near the ends of terminal portal venules. A total of 280 cells were observed *in vivo* during 15 to 90 minutes after injection ($n = 5$ mice), at which time only 1 cell had begun the process of extravasation; all other observed cells were wholly intravascular (Figure 1a). A total of 185 cells were observed *in vivo* at 3 days after injection ($n = 5$ mice), of which only 1 cell remained completely intravascular, 3 were in the process of extravasation, and all other cells were entirely extravascular. The above numbers were expressed as the percentage of observed cells and multiplied by percent cell survival (see below) to convert the results into percentage of injected cells. Thus, at 90 minutes, 87.3% of the injected B16F1 cells remained completely within the microvasculature, whereas by 3 days, the vast majority of injected cells (82.1%) had extravasated into the surrounding tissue.

Survival of Solitary Cells after Successful Extravasation

We were able to express counts of cells, micrometastases, and tumors relative to the absolute number of cancer cells injected, rather than the number observed at any given time in the tissue, by including reference microspheres with the tumor cell suspension injected into the circulation. This cell accounting assay depends on all of the injected microspheres remaining trapped in the liver over the entire course of the study, and to verify this, additional analyses were performed. We determined the numbers of microspheres per cubic millimeter of tissue at 90 minutes (32.7 ± 19.5 (SD)), 3 days (58.6 ± 12.5), and 13 days (37.6 ± 14.5) after injection, from examination of 30-μm-thick sections of livers from four mice at each time point. These results show that there was no overall loss of microspheres during the experimental period ($P = 0.10$; analysis of variance).

The liver was sampled through its whole thickness by counting cells and microspheres in thick sections to assess cell survival. The total percentages of injected B16F1 cells surviving at 90 minutes, 3 days, and 13 days were 87.4%, 83.4%, and 36.2%, respectively. (The percentage cell survival values obtained by intravital videomicroscopy at 90 minutes and 3 days did not differ significantly from the above values obtained from tissue sections; $P \geq 0.31$.) The 12.6% loss during the first 90 minutes was significant ($P < 0.01$), but the additional 4% loss over the next 3 days was not ($P = 0.21$), suggesting that any early cancer cell loss occurred soon after injection. By day 13, cell survival was significantly lower than at the other two time points ($P < 0.01$), showing that additional loss had occurred after extravasation. Despite this loss, more than one-third of injected cells still remained in the liver at day 13.

At 90 minutes after injection, all surviving cells were found within periportal sinusoids as solitary cells. At both days 3 and 13, most of the injected cells remaining were found in the extravascular tissue as solitary cells, and very few had formed micrometastases or macroscopic tumors (see below). The percentages of injected cells present as solitary cells at the three time points are shown in Figure 2; 87.4% remained at 90 minutes ($n = 5$ mice; the sections used for analysis contained a total of 6271 solitary cells and 1403 reference microspheres), 81.4% remained at day 3 ($n = 5$ mice; 5570 solitary cells, 1299 microspheres), and 36.1% remained at day 13 ($n = 5$ mice; 1445 solitary cells, 836 microspheres). Thus, almost 2 weeks after injection, more than one-third of the cells still survived within the liver as solitary extravasated cells.

Limited Survival of Early Micrometastases

By day 3, some cells had developed into micrometastases, all consisting of 4 to 16 cells (see example, Figure 1b). Although the vast majority of injected cells successfully extravasated (82.1%), only 2.04% began to replicate (Figure 3; $n = 5$ mice, 126 micrometastases). At day 13,

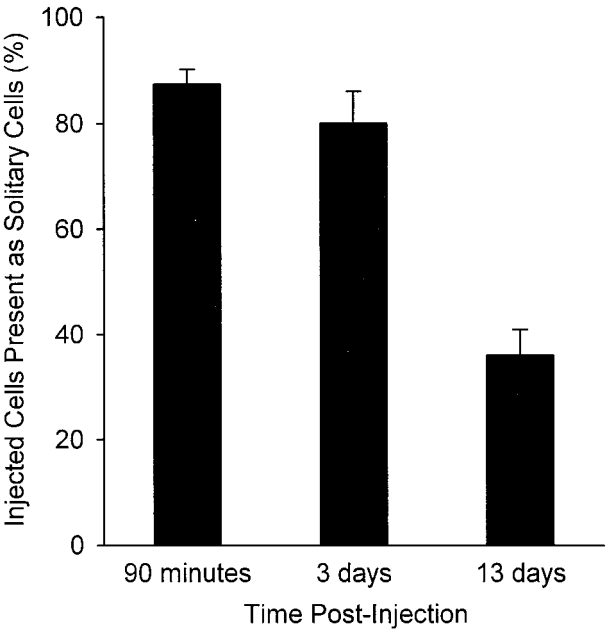

Figure 2. Survival of solitary melanoma cells in mouse liver after intraportal injection, assessed in thick tissue sections by a novel cell accounting technique. The loss of cells during the first 90 minutes was significant ($P < 0.01$), but the additional loss over the next 3 days was not ($P = 0.21$). By day 13, cell survival was significantly lower than at the other two time points ($P < 0.01$) but still amounted to more than one-third of the cells originally injected. Error bars represent SD.

when 36.1% of injected cells were still present in the tissue as solitary cells, only 0.07% of injected cells were present as micrometastases (Figure 3; $n = 5$ mice, 3 micrometastases). Thus, between days 3 and 13 the number of early micrometastases decreased by a factor of 29. In contrast, during this same interval, the number of solitary cells fell by only a factor of 2.3 (Figure 2). These ratios indicate that the rate of loss of micrometastases was more than an order of magnitude greater than that for solitary cells.

The metastasis assay showed that only 0.018% ± 0.017% (SD) of the injected cells had formed macroscopic tumors on the liver surface by day 13 (Figure 3; $n = 8$ mice; numbers of tumors per liver were 4, 4, 5, 49, 65, 69, 72, and 151). To address whether in our model tumors also develop in the interior of the liver, three of the livers (randomly chosen) were grossly sectioned to ~1 mm thick using a scalpel. Forty of these sections (two sides per section) examined under a dissecting microscope showed only 1 tumor in the interior of the liver (not visible by examining the liver surface) *versus* 76 at the surface. This confirms that counting the number of B16F1 tumors on the liver surface gives an accurate picture of the number present in the whole organ.

Dormancy of Solitary Cancer Cells after Extravasation

To determine whether the cancer cells remaining in liver tissue as solitary cells 2 weeks after injection were dormant, we used immunohistochemistry to stain serial tissue sections with (in order): H&E, TUNEL to assess ap-

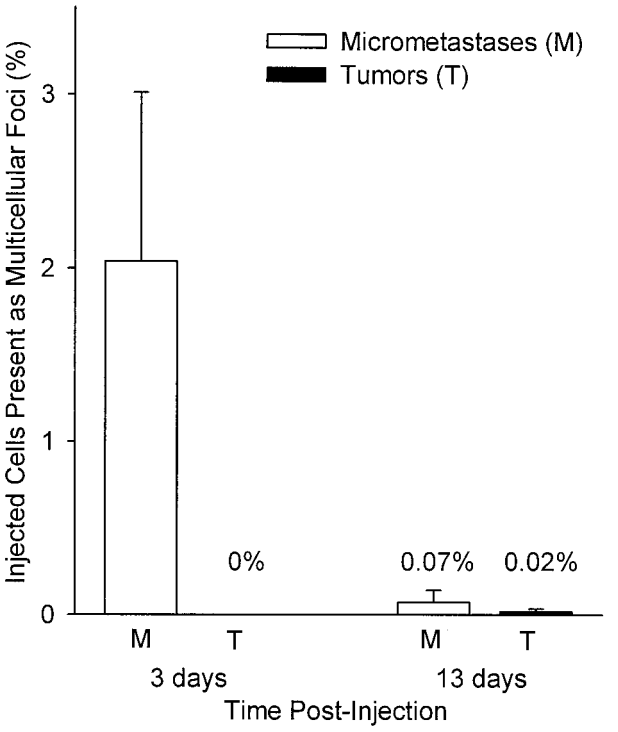

Figure 3. Survival of injected melanoma cells as multicellular foci in liver, assessed in thick sections by the cell accounting technique. Only 2% of injected cells had formed micrometastases (4 to 16 cells) by day 3, and most of these had disappeared by day 13. Only 1 in 100 of the micrometastases, representing 0.02% of injected cells, had continued to grow into macroscopic tumors by day 13 (which virtually all form at the liver surface). Error bars represent SD.

optosis, S100 to identify melanoma cells, and Ki-67 to assess proliferation. When a melanoma cell was identified by S100, the adjacent serial sections were examined to determine whether this cell was undergoing apoptosis or proliferation. The micrographs in Figure 4 show examples of solitary cells (and tumors) stained with S100, TUNEL, and Ki-67. A total of 174 solitary cancer cells were found, and of these, only 5 (3%) stained with TUNEL and 3 (2%) with Ki-67 (Figure 5). Thus, 166 of these solitary cells (95%) showed no evidence of either apoptosis or proliferation, indicating that they were dormant. The sections also showed six small tumors, ranging in size from 0.45 × 0.15 mm to 2.8 × 1.4 mm (consisting of ~200 to 2000 cells in a section). The proportion of cells within these tumors that stained with TUNEL was 6 ± 2.7% (mean ± SD) and for Ki-67 was 90.7 ± 6.8% (Figure 5). Thus, only 3.3% of cancer cells within tumors were dormant, ie, displayed no evidence of either apoptosis or proliferation. This low level of dormancy for cells within tumors stands in marked contrast to the very high level of dormancy (95%) that was found for solitary cells.

Discussion

Traditional approaches to study hematogenous metastasis do not enable one to directly observe the metastatic process *in vivo*, and conclusions often have been based on reasonable inferences instead of primary observations. In the present study we used *in vivo* videomicroscopy in a mouse liver metastasis model, together with a cell accounting technique and immunohistochemistry, to investigate the multistep nature of metastatic inefficiency. The liver is an organ of great clinical importance, as many cancers, especially those of the splanchnic organs (eg, colorectal, pancreatic, and ovarian cancer), metastasize to the liver. This study is the first to quantify the proportions of injected cells remaining at progressive stages of the metastatic process: cell arrest in the microcirculation, extravasation, and growth into early micrometastases and macroscopic tumors.

Our overall findings are summarized as a flow chart in Figure 6, showing the multistep nature of metastatic inefficiency. The majority (>80%) of injected cells survived the initial phase within the circulation and had successfully extravasated by day 3. Very few of these extravasated cells divided and formed colonies; only 1 in 40 had formed micrometastases (4 to 16 cells) by day 3. Furthermore, few of the micrometastases continued to grow; only 1 in 100 micrometastases progressed to form macroscopic tumors by day 13, whereas most micrometastases had disappeared. More than one-third of the extravasated cells were still present in the tissue at day 13, as solitary cancer cells, most of which were dormant. As shown in Figure 5, only 5% of solitary cells were undergoing either proliferation or apoptosis, in contrast to a value of 97% for cells within macroscopic tumors. Loss of injected cells occurred in two phases: a rapid loss of just over 10% within the microvasculature by 90 minutes followed by a slow loss of 50% within the extravascular tissue by 2 weeks (the 4% loss between 90 minutes and 3 days was not statistically significant).

Cancer cell destruction in the microcirculation and an inability to extravasate have been considered rate-limiting steps in metastasis and major contributors to metastatic inefficiency.[4,8,27–29] In studies using nuclear labeling of cells with a radioactive thymidine analogue, rapid destruction of most injected cells has been inferred from residual radioactivity in organs (see, eg, Refs. 5 and 30). However, by direct videomicroscopic observation of individual cancer cells *in vivo*, we have observed such massive destruction of injected cells only when they were labeled with a nuclear stain but not when a cytoplasmic label was used.[12,13] In the present study, individual cells labeled with cytoplasmic fluorescent nanospheres were observed both *in vivo* and in tissue sections, and cell loss within the microcirculation was limited to just over 10%. Furthermore, by 3 days, over 80% of injected cells had successfully extravasated into the tissues. These results are consistent with our previous findings in chick embryo CAM.[11] Thus, our studies indicate that, in both chick CAM and mouse liver, early cell destruction in the microcirculation and an inability of cells to extravasate are not major contributors to metastatic inefficiency.

Contrary to what has been generally thought, only a small percentage of the cancer cells that succeeded in extravasating went on to form tumors. Only 1 in 40 extravasated cells had formed micrometastases by day 3, and the rest remained in liver tissue as solitary cells. This indicates that a major contributor to metastatic ineffi-

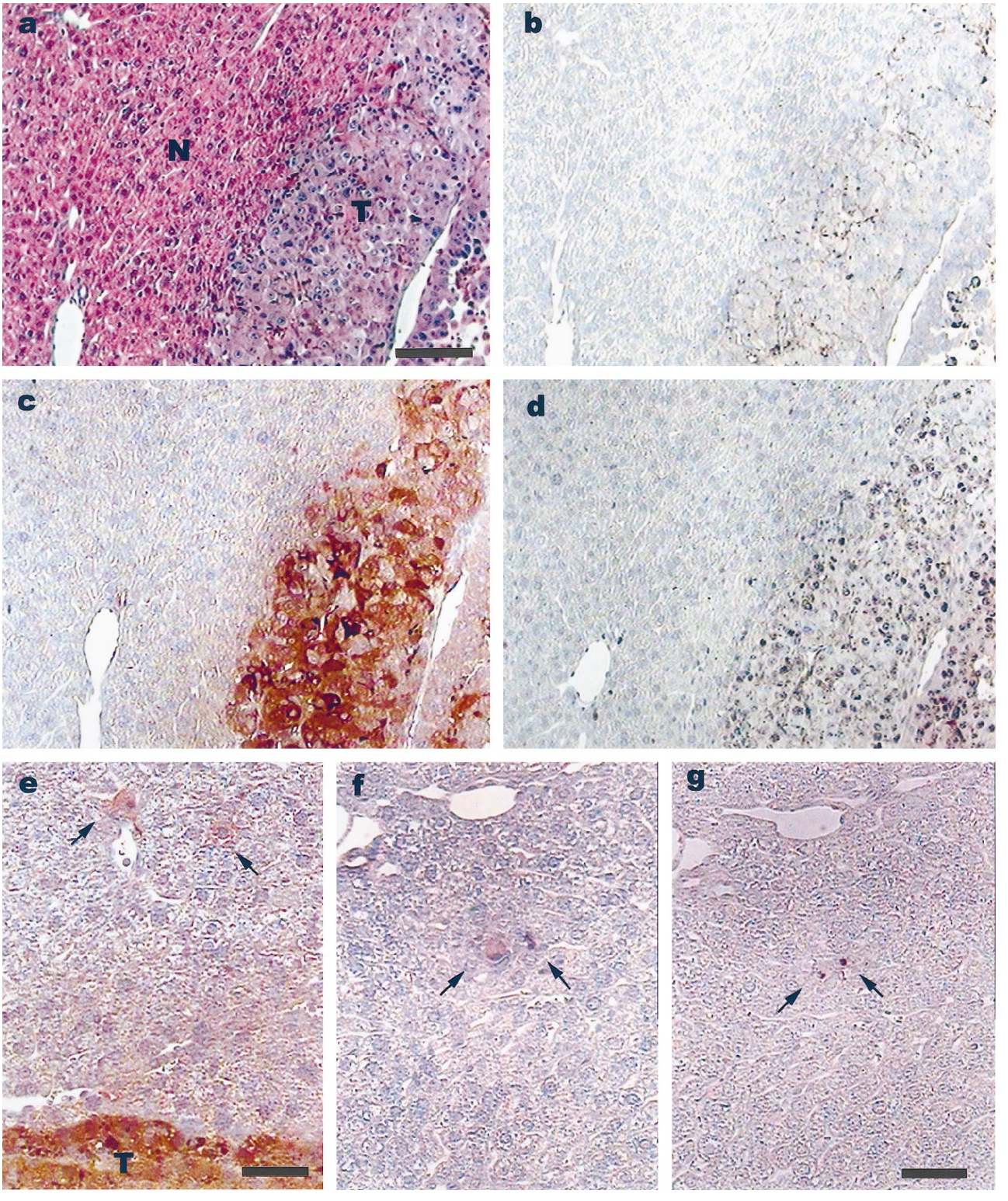

Figure 4. Immunohistochemical staining of liver sections to assess apoptosis or proliferation of melanoma cells at 2 weeks after injection. a–d: Serial sections showing macroscopic tumor (T) and normal tissue (N). Bar, 100 μm. a: Hematoxylin and eosin. b: TUNEL assay shows that very few cells within the tumor were undergoing apoptosis. (The DNAse-positive controls, not shown, exhibited staining of virtually all cell nuclei.) c: S100 Ab identifies melanoma cells, which in this field of view were present only within the tumor. d: Ki-67 Ab shows that most cells within the tumor were proliferating. e: Examples of solitary melanoma cells (→) in normal tissue adjacent to a tumor (T), identified by S100 staining. These solitary cells did not stain with TUNEL or Ki-67 (data not shown), indicating that they were dormant. Bar, 50 μm. f and g: Examples of solitary melanoma cells (→) undergoing apoptosis. Serial sections; bar, 50 μm. Two cells identified by S100 (f) also stained positively with TUNEL (g), indicating apoptosis.

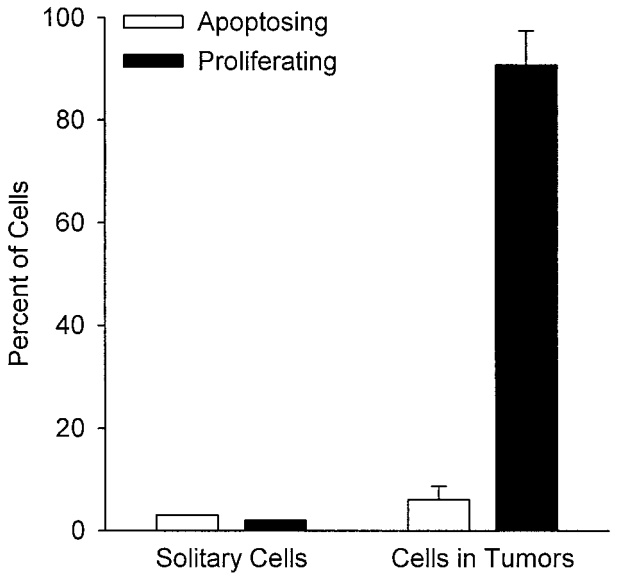

Figure 5. Percentages of melanoma cells undergoing apoptosis (TUNEL stain) or proliferation (Ki-67 stain) for solitary cells *versus* cells in tumors, at 2 weeks after injection. Data obtained by quantification from serial sections (see Figure 4) show dramatic differences in proliferation for solitary cells *versus* cells in tumors but very low levels of apoptosis in both instances. These results indicate that 95% of solitary cells were dormant *versus* only 3% in tumors.

ciency was failure of extravasated cells in the target organ to initiate growth. However, initiation of growth cannot fully account for metastatic inefficiency, as only 1 in 100 of the micrometastases that formed by day 3 actually went on to form macroscopic tumors. Thus, another major contributor to metastatic inefficiency was the failure of micrometastases to continue growth into macroscopic tumors.

What, then, is the fate of solitary cells and micrometastases that do not go on to form tumors? Our results

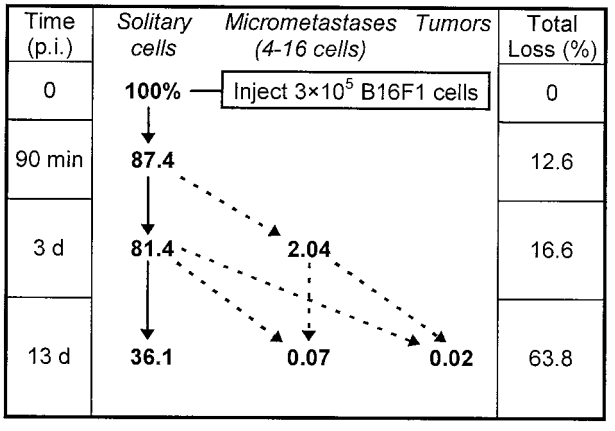

Figure 6. Flow chart summarizing survival data shows the multistep nature of metastatic inefficiency: percentages of injected cells remaining as solitary cells, or forming micrometastases or macroscopic tumors, at different times after injection (p.i.). (At 90 minutes, >85% of injected cells were intravascular, whereas by 3 days, >80% had completed extravasation.) Note the slow loss of solitary cells with time. Dotted arrows indicate possible origins of micrometastases and macroscopic tumors. Two distinct steps after extravasation were principal determinants of metastatic inefficiency: failure of solitary cells to initiate growth and failure of micrometastases to continue growth into macroscopic tumors.

show that, although a slow loss of cells occurred with time, by day 13 over one-third of injected cells remained in the liver as solitary extravasated cells, of which only 5% were undergoing either proliferation or apoptosis. Thus, we conclude that 95% of these solitary cancer cells were dormant. It is conceivable that this large pool of dormant cells had the potential to be activated at some later time, which would be consistent with clinical evidence that human malignancies can recur years after apparently successful treatment of a primary tumor.[31,32] In contrast to the relatively high survival of solitary cancer cells in tissue at day 13, our results show a very low survival for early micrometastases. Only 3.5% of the micrometastases present at day 3 still remained by day 13, and 1% had developed into macroscopic tumors, whereas the remainder had disappeared. This means that the loss of micrometastases occurred at a 10-fold greater rate than the loss of solitary cells, suggesting that cancer cells that begin to divide *in vivo* are much more vulnerable to destruction than solitary cells in an inactive state.

Tumor dormancy is a well established concept, referring to the failure of some small tumors (≤1 to 2 mm diameter) to increase further in size because of an absence of angiogenesis.[33] Recent evidence shows that such dormancy can arise from balanced proliferation and apoptosis within the tumor.[34] Our finding that 95% of the large pool of solitary cancer cells in the liver at 2 weeks were neither proliferating nor undergoing apoptosis represents an additional concept of dormancy, applied to single tumor cells. If these cells have the potential to be activated at a later time and commence growth, they would be analogous to time bombs hidden within the tissue. If this situation also applies clinically, then it will be important to learn how to control these potentially activatable cells. Because these cells have a low proliferative index, they would be unaffected by therapies directed against dividing cells. Growth of tumor cells immediately after extravasation or after a period of cellular dormancy is regulated by a combination of factors inherent to individual cells and the microenvironment in which they are located (eg, growth factors, hormones, extracellular matrix[35–37]). Whether the continued growth of early micrometastases is regulated similarly is not yet clear, but it is known that growth of larger metastases (>1 to 2 mm) depends on angiogenesis[33] as well as immune regulation.[38] Our results point to the initiation and maintenance of growth of micrometastases, as well as activation of dormant solitary cells, as key targets against which therapeutic strategies should be directed.

Acknowledgments

We thank Marsha Grattan and David Huffman for technical assistance and Dr. Alan Tuck (Pathology Department, London Health Sciences Center) for assistance in the analysis of tissue sections.

References

1. Weinstat-Saslow D, Steeg PS: Angiogenesis and colonization in the tumor metastatic process: basic and applied advances. FASEB J 1994, 8:401–407
2. Fidler IJ, Ellis LM: The implications of angiogenesis for the biology and therapy of cancer metastasis. Cell 1994, 79:185–188
3. Liotta LA, Stetler-Stevenson WG: Principles of molecular cell biology of cancer: cancer metastasis. Cancer: Principles and Practice of Oncology. Edited by DeVita VT Jr, Hellman S, Rosenberg SA. Philadelphia, Lippincott, 1993, pp 134–149
4. Weiss L: Metastatic inefficiency. Adv Cancer Res 1990, 54:159–211
5. Fidler IJ: Metastasis: quantitative analysis of the distribution and fate of tumor emboli labeled with ^{125}I-5-iodo-2′-deoxyuridine. J Natl Cancer Inst 1970, 45:773–782
6. Hanna N: Role of natural killer cells in control of cancer metastasis. Cancer Metastasis Rev 1982, 1:45–64
7. Key M: Macrophages in cancer metastasis and their relevance to metastatic growth. Cancer Metastasis Rev 1983, 2:75–88
8. Weiss L: The biomechanics of cancer cell traffic, arrest, and intravascular destruction. Microcirculation in Cancer Metastasis. Edited by Orr FW, Buchanan MR, Weiss L. Boca Raton, FL, CRC Press, 1991, pp 131–144
9. Liotta LA, Steeg PS, Stetler-Stevenson WG: Cancer metastasis and angiogenesis: an imbalance of positive and negative regulation. Cell 1991, 64:327–336
10. Koop S, MacDonald IC, Luzzi K, Schmidt, EE, Morris VL, Grattan M, Khokha R, Chambers AF, Groom AC: Fate of melanoma cells entering the microcirculation: over 80% survive and extravasate. Cancer Res 1995, 55:2520–2523
11. Koop S, Schmidt EE, MacDonald IC, Morris VL, Khokha R, Grattan M, Leone J, Chambers AF, Groom AC: Independence of metastatic ability and extravasation: metastatic *ras*-transformed and control fibroblasts extravasate equally well. Proc Natl Acad Sci USA 1996, 93:11080–11084
12. Chambers AF, MacDonald IC, Schmidt EE, Koop S, Morris VL, Khokha R, Groom AC: Steps in tumor metastasis: new concepts from intravital videomicroscopy. Cancer Metastasis Rev 1995, 14:279–301
13. Morris VL, MacDonald IC, Koop S, Schmidt EE, Chambers AF, Groom AC: Early interactions of cancer cells with the microvasculature in mouse liver and muscle during hematogenous metastasis: videomicroscopic analysis. Clin Exp Metastasis 1993, 11:377–390
14. Fidler IJ: Selection of successive tumor lines for metastasis. Nature 1973, 242:148–149
15. Morris VL, Koop S, MacDonald IC, Schmidt EE, Grattan M, Percy D, Chambers AF, Groom AC: Mammary carcinoma cell lines of high and low metastatic potential differ not in extravasation but in subsequent migration and growth. Clin Exp Metastasis 1994, 12:357–367
16. Weiss L, Nannmark U, Johansson BR, Bagge U: Lethal deformation of cancer cells in the microcirculation: a potential rate regulator of hematogenous metastasis. Int J Cancer 1992, 50:103–107
17. MacPhee PJ, Schmidt EE, Keown PA, Groom AC: Microcirculatory changes in livers of mice infected with murine hepatitis virus: evidence from microcorrosion casts and measurements of red cell velocity. Microvasc Res 1988, 36:140–149
18. Yasumura S, Lin W, Hirabayashi H, Vujanovic NL, Herberman RB, Whiteside TL: Immunotherapy of liver metastases of human gastric carcinoma with interleukin 2-activated natural killer cells. Cancer Res 1994, 54:3808–3816
19. Rudolph AM Heymann MA: The circulation of the fetus in utero: methods for studying distribution of blood flow, cardiac output and organ blood flow. Circ Res 1967, 21:163–184
20. MacPhee PJ, Schmidt EE, Groom AC: Intermittence of blood flow in liver sinusoids, studied by high-resolution in vivo microscopy. Am J Physiol 1995, 269:G692–G698
21. Chambers AF Wilson S: Use of Neo^{R} B16F1 murine melanoma cells to assess clonality of experimental metastases in the immune-deficient chick embryo. Clin Exp Metastasis 1988, 6:171–182
22. Talmadge JE, Wolman SR, Fidler IJ: Evidence for the clonal origin of spontaneous metastases. Science 1982, 217:361–363
23. Talmadge JE, Zbar B: Clonality of pulmonary metastases from the bladder 6 subline of the B16 melanoma studied by Southern hybridization. J Natl Cancer Inst 1987, 78:315–320
24. Gavrieli Y, Sherman Y, Ben-Sasson SA: Identification of programmed cell death in situ via specific labeling of nuclear DNA fragmentation. J Cell Biol 1992, 119:493–501
25. Gerdes J, Li L, Schlueter C, Duchrow M, Wohlenberg C, Gerlach C, Stahmer I, Kloth S, Brandt E, Flad HD: Immunobiochemical and molecular biologic characterization of the cell proliferation-associated nuclear antigen that is defined by monoclonal antibody Ki-67. Am J Pathol 1991, 138:867–873
26. Kindblom LG, Lodding P, Rosengren L, Baudier J, Haglid K: S-100 protein in melanocytic tumors. Acta Pathol Microbiol Immunol Scand A 1984, 92:219–230
27. Stetler-Stevenson WG, Aznavoorian S, Liotta LA: Tumor cell interactions with extracellular matrix during invasion and metastasis. Annu Rev Cell Biol 1993, 9:541–543
28. Nicolson GL: Molecular mechanisms of cancer metastasis: tumor and host properties and the role of oncogenes and suppressor genes. Curr Opin Oncol 1991, 3:75–92
29. Liotta LA, Stetler-Stevenson WG: Tumor invasion and metastasis: an imbalance of positive and negative regulation. Cancer Res 1991, 51:5054s–5059s
30. Fidler IJ, Gersten DM, Riggs CW: Relationship of host immune status to tumor cell arrest, distribution, and survival in experimental metastasis. Cancer 1977, 40:46–55
31. Wheelock EF, Weinhold KJ, Levich J: The tumor dormant state. Adv Cancer Res 1981, 34:107–140
32. Hadfield G: The dormant cancer cell. Br Med J 1954, 2:607–609
33. Folkman J: The role of angiogenesis in tumor growth. Semin Cancer Biol 1992, 3:65–71
34. Holmgren L, O'Reilly MS, Folkman J: Dormancy of micrometastases: balanced proliferation and apoptosis in the presence of angiogenesis suppression. Nature Med 1995, 1:149–153
35. Nicolson GL: Paracrine and autocrine growth mechanisms in tumor metastasis to specific sites with particular emphasis on brain and lung metastasis. Cancer Metastasis Rev 1993, 12:325–343
36. Bates RC, Lincz LF, Burns GF: Involvement of integrins in cell survival. Cancer Metastasis Rev 1995, 14:191–203
37. Radinsky R: Modulation of tumor cell gene expression and phenotype by the organ-specific metastatic environment. Cancer Metastasis Rev 1995, 14:323–338
38. Searle PF, Young LS: Immunotherapy. II. Antigens, receptors, and costimulation. Cancer Metastasis Rev 1996, 15:329–349